Current Optics and Photonics
Vol. 3, No. 5, October 2019, pp. 365-373

ISSN: 2508-7266(Print) / ISSN: 2508-7274(Online)
DOI: https://doi.org/10.3807/COPP.2019.3.5.365

Performance Analysis of Hybrid SIMO-RF/FSO Communication System with Fixed Gain AF Relay

Wenxiao Shi, Kai Kang, Zhuo Wang, and Wei Liu*

College of Communication Engineering, Jilin University, Changchun 130012, PR China

(Received May 7, 2019 : revised June 9, 2019 : accepted July 26, 2019)

This paper investigates the performance of a hybrid single input multiple output radio frequency/free-space optics (SIMO-RF/FSO) communication system. Each SIMO-RF link is modeled as an independent and identically distributed (i.i.d.) Rayleigh distribution, while the FSO link follows a generalized Málaga (M) distribution. Considering the fixed gain amplify-and-forward (AF) relay and misalignment errors, novel expressions for the outage probability (OP), average bit error rate (ABER) and average capacity are derived. Numerical results show that atmospheric turbulence and misalignment errors can seriously impair the system performance, and the hybrid RF/FSO communication system using SIMO-RF links can greatly improve system performance. We also analyze system performance under different types of modulation schemes. Numerical results are verified by Monte Carlo simulations.

Keywords : Free-space optics communication, Hybrid SIMO-RF/FSO communication system, Performance analysis, Fixed gain AF relay
OCIS codes : (010.1290) Atmospheric optics; (010.1330) Atmospheric turbulence; (060.2605) Free-space optical communication; (060.4510) Optical communications

I. INTRODUCTION

Free-space optics (FSO) communications have initially attracted attention because of high rates, excellent security, and unlicensed optical spectra [1]. FSO is widely used in the last-mile access, disaster recovery, etc. [2]. However, the performance of FSO communication systems is severely affected by atmospheric turbulence and misalignment errors [3]. The hybrid radio frequency/free-space optics (RF/FSO) communication system, which is an asymmetric dual-hop relay system, was presented to address the effects of atmospheric turbulence [2].

The amplify-and-forward (AF) relay and decode-and-forward (DF) relay are usually used in the hybrid RF/FSO communication system. The basic principle of AF relay is that the relay node simply amplifies and forwards the signal. In the DF scheme, the relay node not only makes some simple amplification, but also decodes the incoming signal and sends it to the next node after recoding and modulation. In fact, owing to less complexity and simpler facilities, the AF scheme has more advantages in practical applications [4]. The authors studied the performance of the hybrid RF/FSO communication systems using AF and DF relays in [5, 6] and [7], respectively. Moreover, the gain schemes of the relay are divided into fixed gain and variable gain. Among them, the variable gain scheme needs to obtain the full channel state information (CSI), and the fixed gain scheme does not need to. In the hybrid RF/FSO communication system, better communication quality can be achieved by using fixed gain compared to variable gain [8]. In [9] and [10], the research of the hybrid RF/FSO communication system was carried out using fixed gain and variable gain, respectively.

Many models can be used to describe atmospheric turbulence, such as Gamma-Gamma, double generalized Gamma (DGG) and Málaga (M) distribution models. For most papers, FSO atmospheric turbulence links are generally considered to experience a Gamma-Gamma distribution. In

*Corresponding author: jdlw@jlu.edu.cn, ORCID 0000-0001-8078-1879
Color versions of one or more of the figures in this paper are available online.

[11, 12], Nakagami-m, κ-μ or η-μ fading for RF link and DGG, Gamma-Gamma atmospheric turbulence for FSO link are studied. The M fading model can be used to represent the Gamma-Gamma, the K, and the negative exponential distributions under certain conditions and is suitable for different atmospheric turbulence scenarios. In [13], the authors derive the expressions of outage probability (OP) and average bit error rate (ABER) performance under the M distributed turbulence FSO link. The study in [14] investigates the performance of hybrid RF/FSO communication systems in 5G backhaul networks, including the OP, the ABER, and the capacity performance. The Rician distribution for RF channel and the M distribution for FSO fading channel are considered. The hybrid RF/FSO communication systems are investigated in [15] and [16], where the FSO links follow the M distribution.

Most of the works consider RF and FSO hops with single antenna and single aperture. The authors in [17] studied the hybrid RF/FSO communication system with single input multiple output RF (SIMO-RF) links and multiple input multiple output FSO (MIMO-FSO) links. In [18, 19], OP and ABER expressions of the hybrid SIMO-RF/FSO communication relay system are investigated. The relays are assumed to adopt the variable gain AF scheme. The SIMO-RF hops can provide receive diversity advantage at the relay. However, fixed gain AF relay is rarely discussed in the hybrid SIMO-RF/FSO communication relay system.

In this work, a hybrid SIMO-RF/FSO communication system with a fixed gain AF relay is presented. The RF links and FSO link are considered to be subject to Rayleigh fading and M fading, respectively. The relay adopts the maximum ratio combination (MRC) scheme to process the received signal. The expressions of OP, ABER and average capacity considering misalignment errors are derived. The main contributions are as follows:

- We introduce a fixed gain AF relay into the hybrid SIMO-RF/FSO communication system and compare it to the traditional single input single output RF/FSO (SISO-RF/FSO) communication system.
- The cumulative density functions (CDF) of end-to-end SNR is provided, on this basis, novel closed-form expressions for OP, ABER and average capacity are derived by using the correlation operation of the Meijer's G function.
- Numerical analyses are given on the proposed system with the impact of number of RF links, misalignment errors, atmospheric conditions, type of modulation schemes. The numerical results are verified by Monte Carlo simulations.

The remainder of this work is organized as follows. In Section II, the system and channel model of the proposed system are introduced. We obtain the statistical analysis of end-to-end SNR considering misalignment errors in Section III. In Section IV, the novel expressions of OP, ABER and average capacity are derived. Section V illustrates several numerical results. And the main conclusion is presented in Section VI.

II. SYSTEM AND CHANNEL MODEL

A hybrid SIMO-RF/FSO communication system is shown in Fig. 1. In this system, the SIMO technology is applied on the RF links, and the source node S uses a single antenna to transmit signals. The relay node R is equipped with L receiving antennas for RF reception and a single transmitting aperture for FSO transmission. The L receiving antennas receive the same independent RF signal. Moreover, the relay R adopts the MRC scheme and fixed gain AF scheme to process singles. A receiving aperture is installed at the destination node D to receive the optical signal from the relay. The original RF signal arrives at the node D after S-R hop and R-D hop. Rayleigh fading channel is considered for SIMO-RF links, and the FSO link follows the M distribution.

2.1. System Model

For the S-R hop, the relay R receiver employs L receiving antennas to receive signal and utilizes MRC scheme to process the received signal. The processed signal is given by

$$r_R = \sum_{l=1}^{L} w_l \left(h_l s + n_l \right), \tag{1}$$

where s is the RF signal sent by the node S, w_l denotes the receive beamforming coefficient at the lth relay receiving antenna, h_l is the lth channel coefficient and n_l represents the additive white Gaussian noise (AWGN).

For the R-D hop, after using the subcarrier intensity modulation (SIM) scheme at the relay, the optical signals transmitted can be expressed as

$$S_R = G(1 + \eta r_R), \tag{2}$$

where η is the electrical-optical conversion coefficient, and G represents the size of the fixed gain. At the destination node D, the optical signal received can be obtained as

$$r_D = IG[1 + \eta \sum_{l=1}^{L} w_l \left(h_l s + n_l \right)] + n_D, \tag{3}$$

where I is the irradiance at R-D hop and n_D is the AWGN.

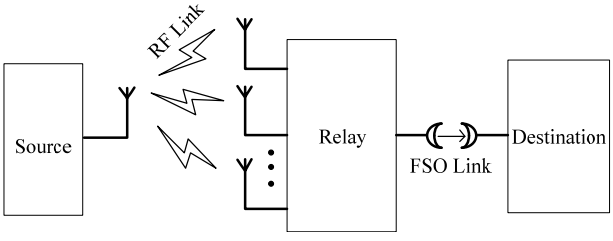

FIG. 1. Hybrid SIMO-RF/FSO communication system.

2.2. RF Channel Model

$\gamma_{RF,l}$ (l =1, ..., L) represents the instantaneous SNR on the lth RF link between node S and node D. Rayleigh fading is considered for each RF link, and the probability density functions (PDF) can be obtained in [20]

$$f_{\gamma_{RF,l}}(\gamma)=\frac{1}{\bar{\gamma}_{RF}}\exp\left(-\frac{\gamma}{\bar{\gamma}_{RF}}\right), \tag{4}$$

where $\bar{\gamma}_{RF}$ is the expectation of $\gamma_{RF,l}$, and we assume that $\gamma_{RF,l}=\bar{\gamma}_{RF}\|h_{SR}\|^2$ is an i.i.d. random variable (RVs) and h_{SR} is the signal fading amplitude.

For the MRC scheme, the instantaneous SNR of the RF link γ_{RF} is the sum of L RVs $\gamma_{RF,l}$ subjected to exponential distribution. γ_{RF} can be calculated as [17]

$$\gamma_{RF}=\sum_{l=1}^{L}\gamma_{RF,l}. \tag{5}$$

For Rayleigh fading models, the Laplace transform method is used to derive the sum of i.i.d RVs which subjected to exponential distribution, which can help us reduce the difficulty of derivation. The moment generating function (MGF) of $\gamma_{RF,l}$ can be expressed as $M_{\gamma_{RF,l}}(s)=\left(1-s\bar{\gamma}_{RF}\right)^{-1}$ [21], so the MGF of γ_{RF} can be $M_{\gamma_{RF}}(s)=\prod_{l=1}^{L}M_{\gamma_{RF,l}}(s)=\left(1-s\bar{\gamma}_{RF}\right)^{-L}$. After taking inverse Laplace transform to $M_{\gamma_{RF}}(s)$, the PDF of γ_{RF} can be derived as

$$f_{\gamma_{RF}}(\gamma_{RF})=\frac{1}{\Gamma(L)}\left(\frac{1}{\bar{\gamma}_{RF}}\right)^{L}\gamma_{RF}^{L-1}\exp\left(-\frac{\gamma_{RF}}{\bar{\gamma}_{RF}}\right), \tag{6}$$

where $\Gamma(\cdot)$ is the Gamma function and $\Gamma(x)=\int_0^{+\infty}t^{x-1}e^{-t}dt$.

Further, CDF of γ_{RF} can be given as

$$F_{\gamma_{RF}}(\gamma_{RF})=1-\exp\left(-\frac{\gamma_{RF}}{\bar{\gamma}_{RF}}\right)\sum_{l=0}^{L-1}\frac{1}{l!}\left(\frac{\gamma_{RF}}{\bar{\gamma}_{RF}}\right)^{l}. \tag{7}$$

2.3. FSO Channel Model

In R-D hop, we use the FSO link to transmit optical signals. Atmospheric turbulence and misalignment errors can seriously affect the transmission quality of optical signals in the atmosphere. In this paper, a heterodyne detection (HD) scheme is used to detect FSO signals. The M channel model is introduced to describe the atmospheric turbulence of the FSO channel. The M fading model can be used to represent the Gamma-Gamma, the K, and the negative exponential distributions under certain conditions and is suitable for different atmospheric turbulence scenarios.

The PDF of the irradiance I_a for M model is given as follows [14]

$$f_{I_a}(I_a)=\chi\sum_{k=1}^{\beta}a(k)I_a^{\frac{a+k}{2}-1}K_{a-k}\left(2\sqrt{\frac{\alpha\beta I_a}{\tau\beta+\Omega'}}\right), \tag{8}$$

where α and β are used to represent atmospheric turbulence intensity, $K_\psi(\cdot)$ is the ψ order modified Bessel function of the second kind, τ is the average power of the scattering component received by off-axis eddies, Ω' denotes the average power from the coherent contributions [14]. Other parameters in Eq. (8) are defined as

$$\chi=\frac{2\alpha^{\frac{\alpha}{2}}}{\tau^{1+\frac{\alpha}{2}}\Gamma(\alpha)}\left(\frac{\tau\beta}{\tau\beta+\Omega'}\right)^{\beta+\frac{\alpha}{2}},\tau=2b_0(1-\rho), \tag{9}$$

$$\mathrm{a}(k)=\binom{\beta-1}{k-1}\frac{(\tau\beta+\Omega')^{1-\frac{k}{2}}}{(k-1)!}\left(\frac{\Omega'}{\tau}\right)^{k-1}\left(\frac{\alpha}{\beta}\right)^{\frac{k}{2}}, \tag{10}$$

$$\Omega'=\Omega+2\rho b_0+2\sqrt{2b_0\rho\Omega}\cos(\phi_1-\phi_2), \tag{11}$$

where $\binom{m}{n}$ denotes the binomial coefficient, $2b_0$ is the average power of the total scatter component, Ω is the average power of the LOS component. ϕ_1 and ϕ_2 are the phases of the LOS component and the coupled-to-LOS component. ρ is a number between 0 and 1, and other channel models can be generated by setting the value of ρ and Ω' for M distribution. By setting $\rho=1$, $\Omega'=1$ and $\rho=0$, $\Omega=0$ or $\beta=1$, M distribution can be transformed into Gamma-Gamma and K distributions, respectively.

Assume that the system is affected by misalignment errors, the PDF of the misalignment errors coefficient I_m can be given as [22]

$$f_{I_m}(I_m)=\frac{\xi^2}{A_0^{\xi^2}}I_m^{\xi^2-1},\ 0\le I_m\le A_0, \tag{12}$$

where ξ is used to measure the misalignment error and denotes the ratio between the equivalent beam radius and the misalignment errors displacement standard deviation in the receiver [22]. When ξ tends to be positive infinity, the system does not have misalignment errors. $A_0=\left[erf(v)\right]^2$ is misalignment loss that is a constant, $erf(z)=\frac{2}{\sqrt{\pi}}\int_0^z e^{-t^2}dt$ is the error function, $v=\sqrt{\pi}a/\left(\sqrt{2}\omega_z\right)$, a is the radius of the detection aperture and ω_z is the beam waist.

The path loss I_p is considered a constant when weather conditions and link distance are determined. The joint distribution of $I=I_aI_mI_p$ can be expressed as

$$f_I(I) = \int_{I/(I_p A_0)}^{\infty} f_{I_a}(I_a) f_{I|I_a}(I \mid I_a)\, dI_a = \int_{I/(I_p A_0)}^{\infty} f_{I_a}(I_a) \frac{I}{I_a I_p} f_m\left(\frac{I}{I_a I_p}\right) dI_a . \quad (13)$$

We utilize Eq. (03.04.26.0008.01) in [23] to rewrite the modified Bessel function on Eq. (8) and using Eq. (13), the PDF of I can be obtained as

$$f_I(I) = \frac{\xi^2 \chi}{2I} \sum_{k=1}^{\beta} a(k) \Theta^{-\frac{\alpha+k}{2}} G_{1,3}^{3,0}\left(\frac{\Theta I}{I_p A_0} \middle| \begin{matrix} \xi^2+1 \\ \xi^2, \alpha, k \end{matrix} \right), \quad (14)$$

where $\Theta = \frac{\alpha\beta}{\tau\beta + \Omega'}$, and $G_{p,q}^{m,n}(\cdot)$ is the Meijer's G function. For the HD detection scheme, the PDF of the instantaneous SNR of FSO link γ_{FSO} is given as [24]

$$f_{\gamma_{FSO}}(\gamma_{FSO}) = \frac{\xi^2 \chi}{2\gamma_{FSO}} \sum_{k=1}^{\beta} a(k) \Theta^{-\frac{\alpha+k}{2}} G_{1,3}^{3,0}\left(B\frac{\gamma_{FSO}}{\bar{\gamma}_{FSO}} \middle| \begin{matrix} \xi^2+1 \\ \xi^2, \alpha, k \end{matrix} \right), \quad (15)$$

where $B = \frac{\xi^2 \Theta(\tau + \Omega')}{\xi^2 + 1}$, and $\bar{\gamma}_{FSO}$ is the average electrical SNR of the FSO link.

Then we can get the CDF of γ_{FSO} as

$$F_{\gamma_{FSO}}(\gamma_{FSO}) = \frac{\xi^2 \chi}{2} \sum_{k=1}^{\beta} a(k) \Theta^{-\frac{\alpha+k}{2}} G_{2,4}^{3,1}\left(\frac{B\gamma_{FSO}}{\bar{\gamma}_{FSO}} \middle| \begin{matrix} 1, \xi^2+1 \\ \xi^2, \alpha, k, 0 \end{matrix} \right). \quad (16)$$

III. STATISTICAL ANALYSIS

For the fixed gain AF relay system, the end-to-end instantaneous SNR γ can be given as [25]

$$\gamma = \frac{\gamma_{RF}\gamma_{FSO}}{\gamma_{FSO} + C}, \quad (17)$$

where C represents the size of fixed gain and is assumed that $C = 1$ in the following derivation.

The CDF of γ can be calculated as

$$F_{\gamma_{e2e}}(\gamma) = \Pr\left[\frac{\gamma_{RF}\gamma_{FSO}}{\gamma_{FSO}+1} < \gamma \right] = \int_0^{\infty} \Pr\left[\frac{\gamma_{RF}\gamma_{FSO}}{\gamma_{FSO}+1} < \gamma \middle| \gamma_{FSO} \right] f_{\gamma_{FSO}}(\gamma_{FSO}) d\gamma_{FSO} = \int_0^{\infty} F_{\gamma_{RF}}\left(\frac{1+\gamma_{FSO}}{\gamma_{FSO}} \gamma \right) f_{\gamma_{FSO}}(\gamma_{FSO}) d\gamma_{FSO} . \quad (18)$$

Substituting Eq. (7) into Eq. (18), we have

$$F_{\gamma_{e2e}}(\gamma) = 1 - \int_0^{\infty} \left[\exp\left(-\frac{1+\gamma_{FSO}}{\bar{\gamma}_{RF}\bar{\gamma}_{FSO}} \gamma \right) \sum_{l=0}^{L-1} \frac{1}{l!} \left(\frac{1+\gamma_{FSO}}{\bar{\gamma}_{RF}\bar{\gamma}_{FSO}} \gamma \right)^l \right] f_{\gamma_{FSO}}(\gamma_{FSO}) d\gamma_{FSO} . \quad (19)$$

By using the binomial expansion Eq. (1.111) in [26], Eq. (19) can be rewritten as

$$F_{\gamma_{e2e}}(\gamma) = 1 - \int_0^{\infty} \left[\exp\left(-\frac{\gamma}{\bar{\gamma}_{RF}} \right) \exp\left(-\frac{\gamma}{\bar{\gamma}_{RF}\bar{\gamma}_{FSO}} \right) \times \sum_{l=0}^{L-1} \sum_{r=0}^{l} \frac{1}{r!(l-r)!} \gamma_{FSO}^{-r} \left(\frac{\gamma}{\bar{\gamma}_{RF}} \right)^l \right] f_{\gamma_{FSO}}(\gamma_{FSO}) d\gamma_{FSO} . \quad (20)$$

Substituting Eq. (15) into Eq. (20), Eq. (20) can be simplified as

$$F_{\gamma_{e2e}}^{PE}(\gamma) = 1 - \frac{\xi^2 \chi}{2} \exp\left(-\frac{\gamma}{\bar{\gamma}_{RF}} \right) \sum_{l=0}^{L-1} \sum_{r=0}^{l} \sum_{k=1}^{\beta} \frac{1}{r!(l-r)!} \left(\frac{\gamma}{\bar{\gamma}_{RF}} \right)^l a(k) \Theta^{-\frac{\alpha+k}{2}} \times I_1, \quad (21)$$

where I_1 is defined as

$$I_1 = \int_0^{\infty} \gamma_{FSO}^{-r-1} \exp\left(-\frac{\gamma}{\bar{\gamma}_{RF}\gamma_{FSO}} \right) G_{1,3}^{3,0}\left(B\frac{\gamma_{FSO}}{\bar{\gamma}_{FSO}} \middle| \begin{matrix} \xi^2+1 \\ \xi^2, \alpha, k \end{matrix} \right) d\gamma_{FSO} . \quad (22)$$

Now, using Eq. (11) in [27], the exponential function can use the Meijer's G function representation, i.e.,

$$\exp(-x) = G_{1,0}^{0,1}\left(\frac{1}{x} \middle| \begin{matrix} 1 \\ - \end{matrix} \right) = G_{0,1}^{1,0}\left(x \middle| \begin{matrix} - \\ 0 \end{matrix} \right). \quad (23)$$

Then, with the help of Eq. (07.34.16.0002.01) in [28], we can rewrite I_1 as

$$I_1 = \int_0^{\infty} \gamma_{FSO}^{-r-1} G_{1,0}^{0,1}\left(\frac{\bar{\gamma}_{RF}}{\gamma} \gamma_{FSO} \middle| \begin{matrix} 1 \\ - \end{matrix} \right) G_{1,3}^{3,0}\left(B\frac{\gamma_{FSO}}{\bar{\gamma}_{FSO}} \middle| \begin{matrix} \xi^2+1 \\ \xi^2, \alpha, k \end{matrix} \right) d\gamma_{FSO} . \quad (24)$$

Using Eq. (07.34.21.0013.01) in [28], Eq. (24) can be calculated as

$$I_1 = \left(\frac{\bar{\gamma}_{RF}}{\gamma} \right)^r G_{1,4}^{4,0}\left(\frac{B\gamma}{\bar{\gamma}_{RF}\bar{\gamma}_{FSO}} \middle| \begin{matrix} \Delta 1 \\ \Delta 2 \end{matrix} \right), \quad (25)$$

where $\Delta 1 = \xi^2 + 1$ and $\Delta 2 = \xi^2, \alpha, k, r$.

Substituting Eq. (25) into Eq. (21) and simplifying, the novel closed-form expression of the CDF of γ with misalignment errors is

$$F_{\gamma_{e2e}}(\gamma) = 1 - \frac{\xi^2 \chi}{2} \exp\left(-\frac{\gamma}{\bar{\gamma}_{RF}} \right) \sum_{l=0}^{L-1} \sum_{r=0}^{l} \sum_{k=1}^{\beta} \frac{1}{r!(l-r)!} \left(\frac{\gamma}{\bar{\gamma}_{RF}} \right)^{l-r} a(k) \Theta^{-\frac{\alpha+k}{2}} G_{1,4}^{4,0}\left(\frac{B\gamma}{\bar{\gamma}_{RF}\bar{\gamma}_{FSO}} \middle| \begin{matrix} \Delta 1 \\ \Delta 2 \end{matrix} \right). \quad (26)$$

IV. PERFORMANCE ANALYSIS

In this section, the expressions of OP, ABER and average capacity with misalignment errors are derived for the system mentioned above. Furthermore, different modulation schemes are investigated for the ABER performance of system.

4.1. Outage Probability

The OP is an evaluation indicator of system performance. When γ is lower than a certain SNR threshold γ_{th}, an outage event is generated. This event is probabilistically distributed, depending on the average SNR of the link and its channel fading distribution model [20]. The outage probability can be given as [29]

$$P_{out} = \Pr\{\gamma < \gamma_{th}\} = F_{\gamma_{e2e}}(\gamma_{th}). \tag{27}$$

The expressions of the OP can be obtained by setting $\gamma=\gamma_{th}$ in Eq. (26).

4.2. Average Bit Error Rate

Another significant indicator used to evaluate the performance of a communication system is ABER. The expression of the ABER is given in [29] as

$$\overline{P}_b = \frac{q^p}{2\Gamma(p)} \int_0^\infty \exp(-q\gamma)\gamma^{p-1} F_{\gamma_{e2e}}(\gamma) d\gamma, \tag{28}$$

where p and q are the parameters which can be selected in Table 1 for different modulation schemes [29].

Considering the impact of misalignment errors and substituting Eq. (26) into Eq. (28), the expression of ABER for system can be expressed as

$$\overline{P}_b = \frac{1}{2} - \frac{q^p \xi^2 \chi}{4\Gamma(p)} \sum_{l=0}^{L-1} \sum_{r=0}^{l} \sum_{k=1}^{\beta} \frac{1}{r!(l-r)!} \left(\frac{1}{\overline{\gamma}_{RF}}\right)^{l-r} a(k)\Theta^{-\frac{\alpha+k}{2}} \times I_2, \tag{29}$$

where I_2 is the definite integral as

$$I_2 = \int_0^\infty \gamma^{l-r+p-1} \exp\left[-\left(q+\frac{1}{\overline{\gamma}_{RF}}\right)\gamma\right] G_{1,4}^{4,0}\left(\frac{B\gamma}{\overline{\gamma}_{RF}\overline{\gamma}_{FSO}}\middle|\begin{matrix}\Delta 1\\ \Delta 2\end{matrix}\right) d\gamma. \tag{30}$$

TABLE 1. Parameters of binary modulations

Modulation scheme	p	q
Coherent Binary Frequency Shift Keying (CBFSK)	0.5	0.5
Non-Coherent Binary Frequency Shift Keying (CBPSK)	0.5	1
Coherent Binary Phase Shift Keying (NBFSK)	1	0.5
Differential Binary Phase Shift Keying (DBPSK)	1	1

Then we can use Eq. (07.34.21.0088.01) in [28] to calculate Eq. (30). After some manipulation, we have

$$I_2 = \left(q+\frac{1}{\overline{\gamma}_{RF}}\right)^{r-l-p} G_{2,4}^{4,1}\left(\frac{B}{\overline{\gamma}_{RF}\overline{\gamma}_{FSO}\left(q+\frac{1}{\overline{\gamma}_{RF}}\right)}\middle|\begin{matrix}1+r-l-p,\Delta 1\\ \Delta 2\end{matrix}\right). \tag{31}$$

Substituting Eq. (31) into Eq. (29), the ABER corresponding to the misalignment errors can be obtained as

$$\overline{P}_b = \frac{1}{2} - \frac{q^p \xi^2 \chi}{4\Gamma(p)} \sum_{l=0}^{L-1} \sum_{r=0}^{l} \sum_{k=1}^{\beta} \frac{1}{r!(l-r)!} \left(\frac{1}{\overline{\gamma}_{RF}}\right)^{l-r} a(k)\Theta^{-\frac{\alpha+k}{2}} \left(q+\frac{1}{\overline{\gamma}_{RF}}\right)^{r-l-p} \times G_{2,4}^{4,1}\left(\frac{B}{\overline{\gamma}_{RF}\overline{\gamma}_{FSO}\left(q+\frac{1}{\overline{\gamma}_{RF}}\right)}\middle|\begin{matrix}1+r-l-p,\Delta 1\\ \Delta 2\end{matrix}\right). \tag{32}$$

4.3. Average Capacity

The average capacity is an indicator used to measure the ability of a channel to transmit information. The expression of the lower-bound average capacity is given as [29]

$$\overline{C} = \frac{1}{\ln 2} \int_0^\infty \frac{1 - F_{\gamma_{e2e}}(\gamma)}{1+\gamma} d\gamma. \tag{33}$$

With the help of Meijer's G function, $(1+\gamma)^{-1}$ can be expressed as $G_{1,1}^{1,1}\left(\gamma\middle|\begin{matrix}0\\ 0\end{matrix}\right)$ [30]. Then, Substituting Eq. (26) into Eq. (33), the expression of average capacity for the system can be expressed as

$$\overline{C} = \frac{\xi^2 \chi}{2\ln 2} \sum_{l=0}^{L-1} \sum_{r=0}^{l} \sum_{k=1}^{\beta} \frac{1}{r!(l-r)!} \left(\frac{1}{\overline{\gamma}_{RF}}\right)^{l-r} a(k)\Theta^{-\frac{\alpha+k}{2}} I_3, \tag{34}$$

where I_3 is defined as

$$I_3 = \int_0^\infty \gamma^{l-r} \exp\left(-\frac{\gamma}{\overline{\gamma}_{RF}}\right) G_{1,1}^{1,1}\left(\gamma\middle|\begin{matrix}0\\ 0\end{matrix}\right) G_{1,4}^{4,0}\left(\frac{B\gamma}{\overline{\gamma}_{RF}\overline{\gamma}_{FSO}}\middle|\begin{matrix}\Delta 1\\ \Delta 2\end{matrix}\right) d\gamma. \tag{35}$$

Then we can use Eq. (6) in [31] and Eq. (20) in [32] to calculate Eq. (35). we can rewrite I_3 in terms of the extended bivariate Meijer's G function (EGBMGF) as

$$I_3 = \gamma_{RF}^{l-r+1} S\left[\begin{matrix}\begin{pmatrix}1 & 0\\ 0 & 0\end{pmatrix}\\ \begin{pmatrix}1 & 1\\ 0 & 0\end{pmatrix}\\ \begin{pmatrix}0 & 4\\ 1 & 0\end{pmatrix}\end{matrix}\middle|\begin{matrix}l-r+1;-\\ 0;0\\ \Delta 1;\Delta 2\end{matrix}\middle|\begin{matrix}\overline{\gamma}_{RF}\\ \\ \dfrac{B}{\overline{\gamma}_{FSO}}\end{matrix}\right], \tag{36}$$

where $S\left[\begin{array}{c|c|c} \begin{bmatrix} m_1 & 0 \\ p_1-m_1 & q_1 \end{bmatrix} & a_1,\cdots,a_{p_1};b_1,\cdots,b_{q_1} & \\ \begin{pmatrix} m_2 & n_2 \\ p_2-m_2 & q_2-n_2 \end{pmatrix} & c_1,\cdots,c_{p_2};d_1,\cdots,d_{q_2} & x \\ \begin{pmatrix} m_3 & n_3 \\ p_3-m_3 & q_3-n_3 \end{pmatrix} & e_1,\cdots,e_{p_3};f_1,\cdots,f_{q_3} & y \end{array}\right]$ is the EGBMGF.

Substituting Eq. (36) into Eq. (34), the closed-form expression of the average capacity can be obtained as

$$\overline{C}=\frac{\xi^2\chi\overline{\gamma}_{RF}}{2\ln 2}\sum_{l=0}^{L-1}\sum_{r=0}^{l}\sum_{k=1}^{\beta}\frac{1}{r!(l-r)!}a(k)\Theta^{\frac{\alpha+k}{2}}S\left[\begin{array}{c|c|c} \begin{bmatrix} 1 & 0 \\ 0 & 0 \end{bmatrix} & l-r+1;- & \\ \begin{pmatrix} 1 & 1 \\ 0 & 0 \end{pmatrix} & 0;0 & \frac{B}{\overline{\gamma}_{FSO}} \\ \begin{pmatrix} 0 & 4 \\ 1 & 0 \end{pmatrix} & \Delta 1;\Delta 2 & \end{array}\right]. \quad (37)$$

V. NUMERICAL RESULTS

Based on the expressions derived above, we present and analyze numerical results. FSO links are considered with link lengths of 1 km and wavelength of 785 nm [24]. Both turbulence and misalignment errors are considered, and the FSO channel is modeled as the M distribution whose parameters are set to the similar as in [14, 24]. The parameters ($\alpha=2.296, \beta=2$), ($\alpha=4.2, \beta=3$), and ($\alpha=8, \beta=4$) correspond to three cases of different turbulence scenes. And, as the values of α and β become smaller, the turbulence of the atmosphere is more serious. Misalignment errors is investigated with $\xi=1$ (i.e., strong misalignment errors) and $\xi=6$ (i.e., weak misalignment errors). We set the other parameters as $\Omega=0$, $b_0=0.5$, φ_1 - $\varphi_2=\pi/2$, $\rho=1$ [33]. To simplify the analysis, it is usually assumed that $\overline{\gamma}_{RF}=\overline{\gamma}_{FSO}$ [19]. The expressions for OP, ABER and average capacity are demonstrated and verified by Monte Carlo simulations. All simulation results are generated using 5×10^6 samples/SNR value.

For SIMO-RF links, we generate 5×10^6 random variables which subject to Rayleigh distribution to simulate signal fading amplitude h_{SR} of each RF link. Based on $\gamma_{RF,l}=\overline{\gamma}_{RF}\|h_{SR}\|^2$, the instantaneous SNR of each RF link is expressed. Then we superimpose them according to Eq. (5) to simulate the instantaneous SNR of SIMO-RF links γ_{RF}. For FSO links, we generate 5×10^6 M distribution random variables and misalignment errors random variables. Misalignment errors random variables are needed whose PDF is given as Eq. (12). We multiple these random variables and M distribution random variables to simulate optical irradiance I in the presence of misalignment errors. By using $\gamma_{FSO}=\overline{\gamma}_{FSO}\left(\xi^2+1\right)I/[A_0\xi^2(\tau+\Omega')]$ in [24], the instantaneous SNR of the FSO link γ_{FSO} is provided. Then we superimpose them according to Eq. (17), the end-to-end SNR γ is obtained. OP and ABER simulations can be further realized by calculating the probability that the instantaneous SNR falls below the predetermined threshold and the ratio of error transmit symbols to total transmit symbols. The average capacity can be calculated by using $\overline{C}=E\left[\log_2(1+\gamma)\right]$ in [29].

In Fig. 2, we have investigated the OP of the proposed system in different relay antenna number and misalignment errors. The threshold SNR is assumed to be 10 dB. $L=1$ and $L=2$, 4, 6 represent SISO-RF link and SIMO-RF links, respectively. We set the value of α and β as 4.2 and 3. It can be seen that severe misalignment errors would deteriorate the OP performance and larger value of ξ could provide better OP performance for certain atmospheric conditions. On the other hand, Fig. 2 clearly reflects the improvement in the OP performance of the system for $L=$ 2, 4, 6 when comparing with $L=1$. Under the effect of weak misalignment errors, the OP of the SISO-system can only reach 10^{-3}, however, the OP can be lowered to 10^{-6} when L is larger than 1 at average SNR=40 dB. When L changes from 1 to 2, the OP performance of the system will be greatly improved. However, when L changes from 4 to 6, the improvement of OP performance is not very much and the system becomes more complicated.

Figure 3 demonstrates the OP performance of the system under different turbulence conditions. We assume that the system is under the influence of strong misalignment errors. Even if the average SNR reaches 40 dB, the OP of SISO-system can only reach 10^{-3} when the system is destroyed by the effect of strong misalignment errors. As can be seen from the curves, atmospheric turbulence can obviously degrade the OP performance of the system. As atmospheric turbulence becomes severe, the OP performance will continue to deteriorate. The OP of the system decreases when the number of receiving antennas of the relay node increases. In addition, it can be observed that the numerical results match perfectly with the simulation results.

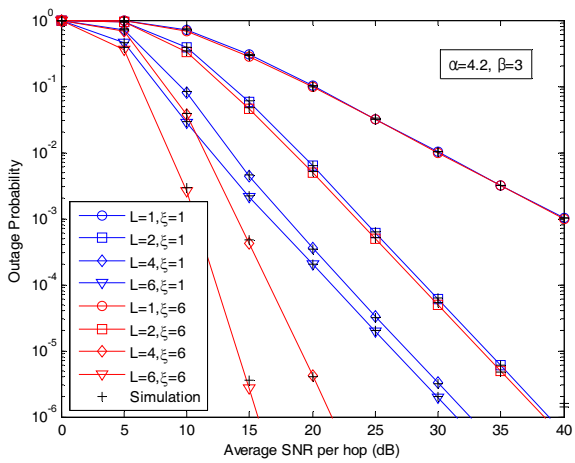

FIG. 2. Outage probability with different relay antenna number and misalignment errors.

Figure 4 shows the ABER performance using CBPSK modulation scheme and misalignment errors is illustrated. We can draw a conclusion similar to Fig. 2. Compared to the traditional SISO relay system, the performance of the hybrid SIMO-RF/FSO communication system is significantly improved. As expected, the ABER performance is very poor when $L = 1$. Specifically, the ABER performance of the SISO-system can only reach a range of 10^{-4} to 10^{-5} at 40 dB average SNR, however, the ABER of the SIMO-RF/FSO system drops below 10^{-6} before the average SNR reaches 30 dB. Furthermore, the ABER performance of the system is greatly improved with the influence of weak misalignment errors. As L continues to increase, the improvement of ABER performance continues to decrease and the complexity of the system increases. Therefore, it is recommended that L is between 2 and 4 in practical applications.

In Fig. 5, we assume relay antenna number $L = 1$ and $L = 3$, the ABER performance under different turbulence conditions is presented. Misalignment errors are investigated with $\xi = 1$. It is demonstrated that atmospheric turbulence can degrade the ABER performance of the system. When the atmospheric turbulence changes from weak to strong, the ABER performance is seriously degraded. Under the condition of weak atmospheric turbulence, the ABER performance of the system can reach below 10^{-6} with $L = 3$.

Figure 6 depicts the ABER performance corresponding to different modulation methods (i.e. DBPSK, NBFSK, CBPSK, CBFSK) with $L = 3$. We can conclude that the performance of CBPSK modulation is superior to other modulation methods. We also find that the performance of the system with NBFSK modulation is poor under the same atmospheric turbulence intensity and misalignment errors. However, regardless of the modulation method, the ABER performance can be reduced to 10^{-6} before the average SNR reaches 30 dB under given conditions.

Figure 7 shows the average capacity performance of the hybrid SIMO-RF/FSO communication system with fixed gain AF relay under different relay antenna number and

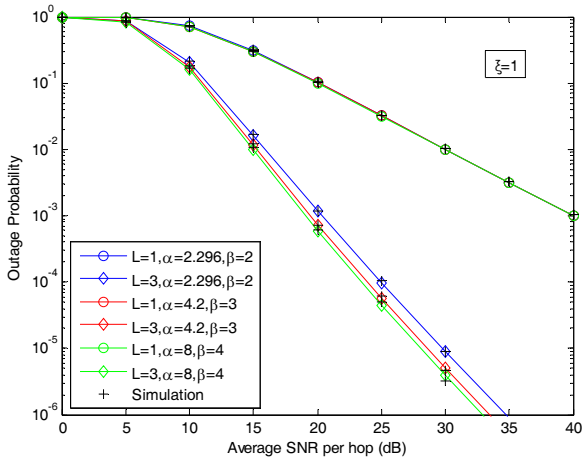

FIG. 3. Outage probability under different turbulence conditions.

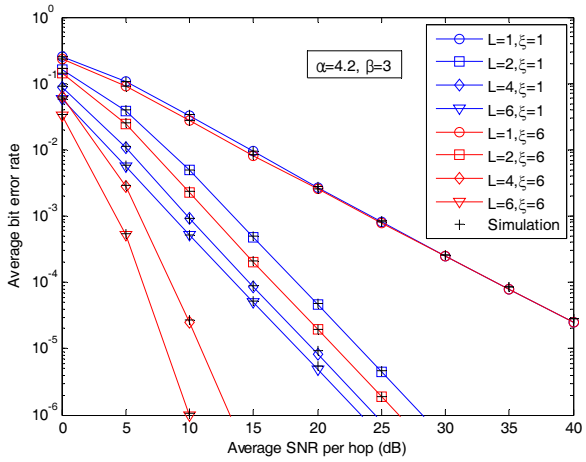

FIG. 4. Average bit error rate with different relay antenna number and misalignment errors.

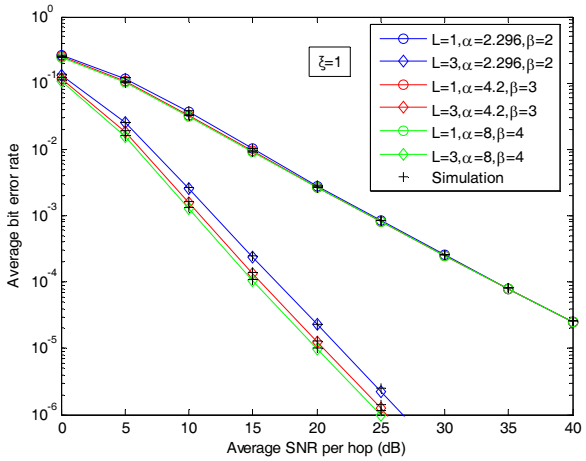

FIG. 5. Average bit error rate under different turbulence conditions.

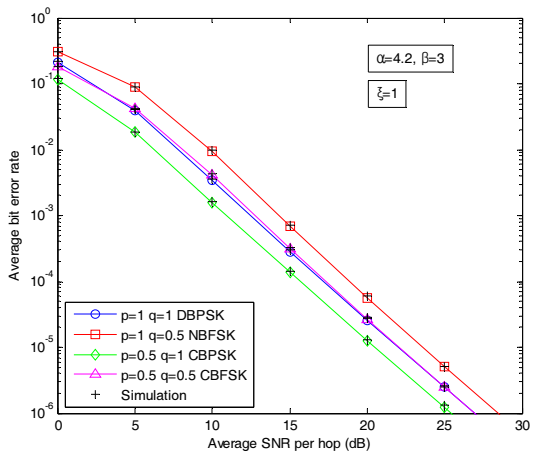

FIG. 6. Average bit error rate with different modulation scheme.

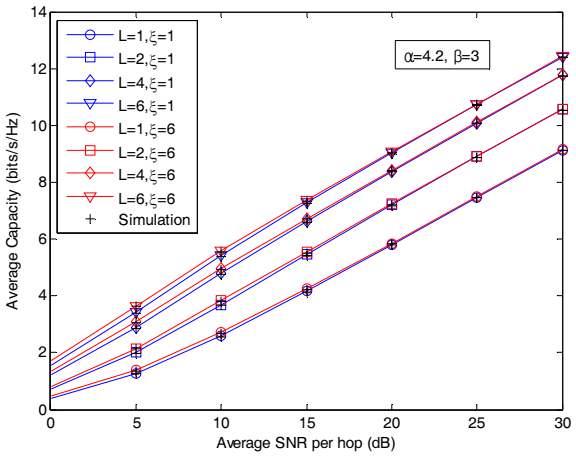

FIG. 7. Average capacity under different relay antenna number and misalignment errors.

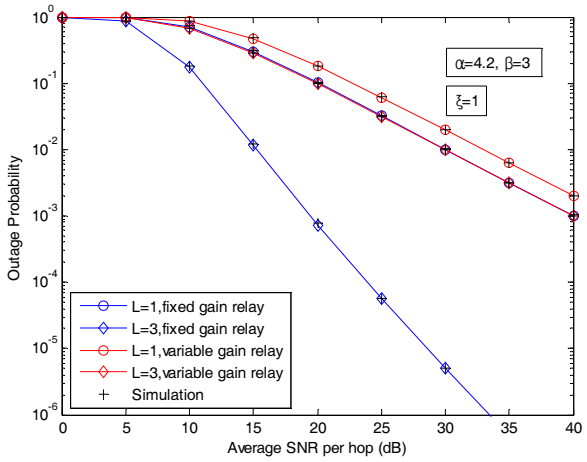

FIG. 8. Outage probability with fixed and variable gain AF relay.

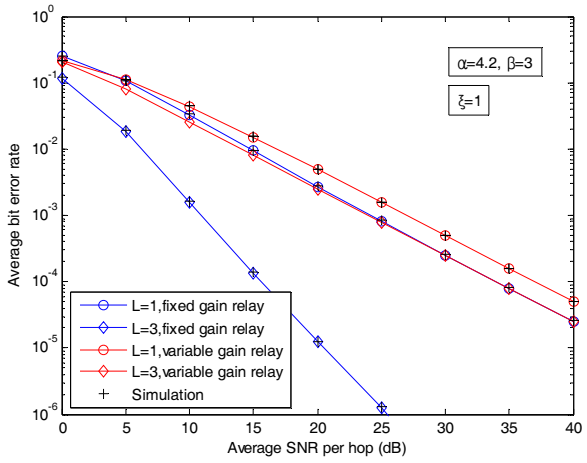

FIG. 9. Average bit error rate with fixed and variable gain AF relay.

misalignment errors. All the capacity numerical results in Fig. 7 closely match with the Monte Carlo simulations results. It is discovered that the average capacity will increase when the relay antenna number becomes greater. Furthermore, misalignment errors can damage the average capacity of the system. The average capacity of the system will decrease when the misalignment errors become stronger. Although using SIMO-RF links increase the complexity of system, the system can achieve higher diversity gain and increase average capacity, which is very meaningful.

In Figs. 8 and 9, the OP and ABER of the hybrid SIMO-RF/FSO communication system with fixed and variable gain AF relay are presented under the same channel conditions. It can be seen clearly that fixed gain relay scheme outperforms variable gain scheme. Moreover, the system performance formula using the DF relay is derived the same as that of the variable gain AF relay, so the performance is the same. Hence, the system with fixed gain AF relay scheme can get better performance.

VI. CONCLUSION

In this work, we investigated and analyzed the performance of the hybrid SIMO-RF/FSO communication system with the fixed gain AF relay. The SIMO-RF links and the FSO link experience Rayleigh fading and M fading, respectively. Considering the presence of misalignment errors, the CDF of end-to-end SNR on the proposed system is obtained, on this basis, the OP, ABER and average capacity performance are obtained in different cases. The numerical results show that using SIMO-RF links can greatly improve system performance. We also demonstrated that both atmospheric turbulence and misalignment errors can markedly deteriorate system OP and ABER performance. However, considering with strong misalignment errors, when the average SNR reaches 40 dB and $L = 2$, the OP and ABER performance can be lowered to 10^{-6}. In addition, the use of SIMO-RF links can increase the diversity gain of the system, and the system can achieve higher system capacity. However, using SIMO-RF links can increase the complexity of system, so it is recommended that the value of L is between 2 and 4 in practical applications.

ACKNOWLEDGMENT

This study was supported by a grant from the National Natural Science Foundation of China (No. 61601195).

REFERENCES

1. V. W. S. Chan, "Free-space optical communications," J. Lightwave Technol. **24**, 4750-4762 (2006).

2. M. A. Khalighi and M. Uysal, "Survey on free space optical communication: A communication theory perspective," IEEE Commun. Surveys Tuts. **16**, 2231-2258 (2014).
3. H. Lei, Z. Dai, K. H. Park, W. Lei, G. Pan, and M. S. Alouini, "Secrecy outage analysis of mixed RF-FSO downlink SWIPT systems," IEEE Trans. Commun. **66**, 6384-6395 (2018).
4. M. O. Hasna and M. S. Alouini, "A performance study of dual-hop transmissions with fixed gain relays," IEEE Trans. Wireless Commun. **3**, 1963-1968 (2004).
5. M. Torabi and R. Effatpanahi, "Performance analysis of hybrid RF-FSO systems with amplify-and-forward selection relaying," Opt. Commun. **434**, 80-90 (2019).
6. E. Balti and M. Guizani, "Mixed RF/FSO cooperative relaying systems with co-channel interference," IEEE Trans. Commun. **66**, 4014-4027 (2018).
7. J. Vellakudiyan, I. S. Ansari, V. Palliyembil, P. Muthuchidambaranathan, and K. A. Qaraqe, "Channel capacity analysis of a mixed dual-hop radio-frequency-free space optical transmission system with Málaga distribution," IET Commun. **10**, 2119-2124 (2016).
8. J. Feng and X. Zhao, "Performance analysis of mixed RF/FSO systems with STBC users," Opt. Commun. **381**, 244-252 (2016).
9. J. Zhao, S. H. Zhao, W. H. Zhao, Y. Liu, and X. Li, "Performance of mixed RF/FSO systems in exponentiated Weibull distributed channels," Opt. Commun. **405**, 244-252 (2017).
10. L. Yang, M. O. Hasna, and X. Gao, "Performance of mixed RF/FSO with variable gain over generalized atmospheric turbulence channels," IEEE J. Sel. Areas Commun. **33**, 1913-1924 (2015).
11. E. Soleimani-Nasab and M. Uysal, "Generalized performance analysis of mixed RF/FSO cooperative systems," IEEE Trans. Wireless Commun. **15**, 714-727 (2016).
12. J. Zhang, L. Dai, Y. Zhang, and Z. Wang, "Unified performance analysis of mixed radio frequency/free-space optical dual-hop transmission systems," J. Lightwave Technol. **33**, 2286-2293 (2015).
13. M. I. Petkovic and Z. Trpovski, "Exact outage probability analysis of the mixed RF/FSO system with variable gain relays," IEEE Photonics J. **10**, 1-14 (2018).
14. P. V. Trinh, T. C. Thang, and A. T. Pham, "Mixed mmWave RF/FSO relaying systems over generalized fading channels with pointing errors," IEEE Photonics J. **9**, 1-14 (2017).
15. V. Palliyembil, J. Vellakudiyan, P. Muthuchidamdaranathan, and T. A. Tsiftsis, "Capacity and outage probability analysis of asymmetric dual-hop RF-FSO communication systems," IET Commun. **12**, 1979-1983 (2018).
16. M. I. Petkovic and Z. Trpovski, "Exact outage probability analysis of the mixed RF/FSO system with variable-gain relays," IEEE Photonics J. **10**, 1-14 (2018).
17. L. Chen and W. Wang, "Multi-diversity combining and selection for relay-assisted mixed RF/FSO system," Opt. Commun. **405**, 1-7 (2017).
18. A. H. A. El-Malek, A. M. Salhab, S. A. Zummo, and M. S. Alouini, "Security-reliability trade-off analysis for multiuser SIMO mixed RF/FSO relay networks with opportunistic user scheduling," IEEE Trans. Wireless Commun. **15**, 5904-5918 (2016).
19. N. Singhal, A. Bansal, and A. Kumar, "Performance evaluation of decode-and-forward-based asymmetric SIMO-RF/FSO system with pointing errors," IET Commun. **11**, 2244-2252 (2017).
20. M. K. Simon and M. S. Alouini, *Digital Communication Over Fading Channels, 2nd ed.* (John Wiley & Sons, New Jersey, 2005).
21. Y. C. Ko, M. S. Alouini, and M. K. Simon, "Outage probability of diversity systems over generalized fading channels," IEEE Trans. Commun. **48**, 1783-1787 (2000).
22. H. G. Sandalidis, T. A. Tsiftsis, and G. K. Karagiannidis, "Optical wireless communications with heterodyne detection over turbulence channels with pointing errors," J. Lightwave Technol. **27**, 4440-4445 (2009).
23. S. Wolfram, *Modified Bessel function of the second kind* (Wolfram: Computation Meets Knowledge, 2001), http://functions.wolfram.com/Bessel-TypeFunctions/BesselK/ (2018).
24. I. S. Ansari, F. Yilmaz, and M. S. Alouini, "Performance analysis of free-space optical links over Málaga (M) turbulence channels with pointing errors," IEEE Trans. Wireless Commun. **15**, 91-102 (2016).
25. A. Papoulis and S. U. Pillai, *Probability, Random Variables, and Stochastic Processes*, 4th ed. (Tata McGraw-Hill Education, Europe, 2002).
26. I. S. Gradshteyn and I. M. Ryzhik, *Table of Integrals, Series, and Products: Corrected and enlarged edition* (Academic Press, London, UK, 2014).
27. V. S. Adamchik and O. I. Marichev, "The algorithm for calculating integrals of hypergeometric type functions and its realization in REDUCE system," in *Proc. The international symposium on Symbolic and algebraic computation* (ACM, Tokyo, Japan, 1990), pp. 212-224.
28. S. Wolfram, *Meijer G-function* (Wolfram: Computation Meets Knowledge, 2001), http://functions.wolfram.com/HypergeometricFunctions/MeijerG/ (2018).
29. E. Zedini, I. S. Ansari, and M. S. Alouini, "Performance analysis of mixed Nakagami- m and Gamma-Gamma dual-hop FSO transmission systems," IEEE Photonics J. **7**, 1-20 (2015).
30. A. M. Mathai and R. K. Saxena, *The H-function With Applications in Statistics and Other Disciplines* (Wiley Eastern, New Delhi, India & Halsted Press, New York, USA, 1978).
31. B. L. Sharma, "Some formulae for generalized function of two variables," Matematički Vesnik **5**, 43-52 (1968).
32. I. S. Ansari, S. Al-Ahmadi, F. Yilmaz, M. S. Alouini, and H. Yanikomeroglu, "A new formula for the BER of binary modulations with dual-branch selection over Generalized-K composite fading channels," IEEE Trans. Commun. **59**, 2654-2658 (2011).
33. A. Jurado-Navas, J. M. Garrido-Balsells, J. F. Paris, and A. Puerta-Notario, "A unifying statistical model for atmospheric optical scintillation" in *Numerical Simulations of Physical and Engineering Processes*, J. Awrejcewicz, ed. (IntechOpen, UK, 2011), Chapter 8.